

External Bremsstrahlung Studies on Films of Lead Monoxide Filled Polycarbonate Composite

V. A. Kandagal¹, B. Lobo^{1*}

¹Department of Physics, Karnatak University's Karnatak Science College, Dharwad-580001, Karnataka, India

ARTICLE INFO

Article history:

Received 13 February 2023

Received in revised form 30 June 2023

Accepted 12 July 2023

Keywords:

External bremsstrahlung

Effective atomic number

Polycarbonate

Lead monoxide

Composite

Beta particles

ABSTRACT

The development of high-Z (high atomic number) radiation shielding materials is vital in order to protect personnel who work with harmful gamma radiation sources. At the same time, the emission of external bremsstrahlung (EB) radiation in those shielding materials when the radiation source emits beta particles as well as gamma radiation is also of prime concern. The production of EB in films of lead monoxide (PbO) loaded polycarbonate (PC) composite at eleven different filler levels (FLs) varying, in terms of weight fraction, from 0.0 % up to 10.0 % were investigated experimentally by using beta particles from strontium-90/yttrium-90 (⁹⁰Sr/⁹⁰Y) radioactive source. A nonlinear relation is observed between EB intensity and target thickness. The effective atomic numbers of the prepared PbO-filled PC composite films (at different FLs) were determined via EB measurements, followed by calculations, and the values obtained were compared with the modified atomic numbers which were determined for the same composite films (at different FLs) using the Markowicz and Van Grieken equation, and it was found that they are in good agreement. Finally, the atomic number dependence of EB in these composite films (PbO-filled PC composites) has been studied. It is obtained that the intensity of EB spectra depends on the square of the atomic number of the target material.

© 2023 Atom Indonesia. All rights reserved

INTRODUCTION

In the last few decades, several techniques involving spin-offs of radiation physics for the study of materials, such as external bremsstrahlung, radiation shielding, neutron scattering, and positron annihilation spectroscopy have drawn the attention of researchers because of their wide applications [1,2]. Bremsstrahlung is defined as the electromagnetic radiation emitted by the deceleration (slowing down) of charged particles like electrons in the electric field of atomic nuclei of the target material. Bremsstrahlung is also known as braking radiation [3,4], and the term itself is the result of combination of two words, namely 'bremsen' and 'strahlung', which means 'to brake' and 'radiation', respectively. The deceleration of beta particles (electrons) in the electric field of the atom (Coulombic field of the nuclei of atoms) results in the emission of radiation in the X-ray and gamma ray regions of the electromagnetic spectrum, with a continuous,

exponentially-decreasing energy distribution, and this process is known as external bremsstrahlung (EB) [5]. The probability of this process depends on the kinetic energy of the incident electrons [6] and the atomic number (Z) of constituents of the target material. The EB emission is high in materials which have high value of Z, because it varies proportionally to Z^2 [7]. The EB spectrum mainly depends on the cross section for interaction of an electron with atoms present in a thick target [8]. In order to produce bremsstrahlung photons, the required energetic electrons can be obtained from radioactive sources (beta particle emitting sources), X-ray tubes (cathode rays inside the X-ray tube, which on impinging the anode or target, results in the production of continuous background or EB radiation, in addition to characteristic or fluorescent X-rays) and electron beam lines (synchrotron radiation) [9].

There are two origins for bremsstrahlung radiation, namely inner or internal bremsstrahlung (IB) and external bremsstrahlung (EB). IB is a low intensity, continuous electromagnetic radiation that is emitted within the transforming atom due to

*Corresponding author.

E-mail address: blaiselobo@kud.ac.in

DOI: <https://doi.org/10.55981/aij.2023.1304>

change in nuclear charge by orbital electron capture or beta particle emission, whereas EB is a continuous electromagnetic radiation existing due to the deflection of charged particles (in general) in the Coulomb field of the nucleus of a medium (stopping material), and this EB process occurs in thick target materials [10]. For the first time, Aston [11] observed the emission of IB radiation during beta decay. The quantum theory for IB, without considering the Coulomb effects for allowed beta transitions, was developed by Knipp and Uhlenbeck [12] and Bloch [13]. These theories are collectively called KUB theory. According to this theory, IB is an electromagnetic, low intensity, and continuous spectrum which includes all kinds of beta decay. The KUB theory was extended by Wang Chang and Falkoff [14] for the foremost and second forbidden transitions. The calculation of IB spectra taking into account the Coulomb effect has been done by Nilsson [15], Spruch and Gold [16], and Lewis and Ford [17]. Ford and Martin [18] developed a theory by calculating possible IB due to detour transitions theoretically, and a good agreement was found between theory and experiment.

The study of EB is of contemporary research interest, as it has applications in many fields, such as astrophysics, plasma physics, food irradiation, radiation shielding, medical diagnostics, and radiation treatment (for example, in the treatment of cancer of liver, bone, muscles, and other organs). Sommerfeld [19] developed a theory for the production of EB by the interaction of nonrelativistic electrons with the Coulomb field of the nucleus (of the target material). Sauter [20], Racah [21], and Bethe and Heitler [22] independently developed theories for EB produced by relativistic incident electrons. However, Tseng and Pratt [23] have found an exact theory using Coulomb field wave function, and it has been extended to an atomic electron field by Seltzer and Berger [24].

External bremsstrahlung radiation has noticeable applications, especially in the medical field. The bremsstrahlung imaging technique is utilized for dosimetry of radionuclide therapies, for which pure beta emitters (such as ^{90}Y) have been used. Bremsstrahlung imaging can trace the tumor sites in the human body. Iodine (^{131}I) is used in thyroid cancer therapy and samarium (^{153}Sm) in osseous metastases therapy [25,26]. In bremsstrahlung radiation therapy [27], the released beta particles interact with body organs such as bone and muscles resulting in the production of EB spectrum with different energies and intensities. Recently, ^{90}Y bremsstrahlung radiation has been used to evaluate the efficiency of radiation therapy by using single photon emission computed

tomography imaging (SPECT) [28], wherein the image obtained gives the distribution of radioactive chemicals (isotopes or tracers) present in the patients body, and the bremsstrahlung spectrum produced by the interaction of beta particles with the tissue. In the bremsstrahlung imaging of human liver, pure beta nuclides have been used in the treatment of malignant diseases, where an image of the liver from beta nuclides is obtained by using bremsstrahlung imaging [29]. In radio-guided surgery, the beta radiation liberates energy in the desired region of the body, up to a few millimeters of tissue. This energy is utilized to locate residual tumors. The limitation of this technique is that the beta radiation locates tumor tissue only in immediate vicinity. To overcome this limitation, bremsstrahlung X-ray photons have been used, because of its high penetration ability [30]. In field-deployable lung counting technique, the measurement of bremsstrahlung radiation produced in the lung by the inhalation of $^{90}\text{Sr}/^{90}\text{Y}$ beta radionuclides is conducted [31]. Bremsstrahlung radiation has been used for irradiation of food [32], in order to prevent or reduce the growth of unwanted biological organisms (in food preservation). Bremsstrahlung gamma images have applications in different areas, such as attenuation correction, scatter correction, quantification and image reconstruction [33], particle accelerators, controlled photonuclear research, shielding of space vehicles [34], plasma physics and astrophysics [35].

Polycarbonate (PC) is a thermoplastic engineering polymer having mass density 1.20 g/cm^3 . PC is commonly used in different fields due to its unique physical and chemical properties, like good transparency, high heat distortion temperature, good mechanical strength [36], high toughness, high impact resistance [37], and the ability to withstand reasonably high temperature (without degradation) [38]. Due to these excellent properties, PC has drawn the attention of researchers and manufacturers, resulting in its applications in different areas such as aerospace, automotive, construction, electronic industries, data storage and telecommunication hardware. It has applications in the manufacture of capacitors, automobile parts such as helmets, head lamp lenses, in vehicles for bullet-proof glasses, bumpers [37], poster protection, bullet resistant windows, displays, security components, construction materials and as a dielectric material in the manufacture of capacitors [37]. It is also used for helmets, automobile parts such as head lamp lenses and bumpers, and bullet-resistant windows and vehicle glass, security components, poster protection, displays, and construction materials [37]. However, even though

PC has many applications, it has several drawbacks, such as strong hydrophobicity, high melt viscosity, notch sensitivity (related to mechanical properties), relative softness, and limited chemical functionality [39]. In order to overcome these limitations of pure PC, the blending of two miscible polymers and doping or filling of organic or inorganic materials have been employed, as these methods help to improve the properties of the resulting (reinforced or filled) composite materials [40-45].

In this paper, PC and PbO have been used as polymer matrix and inorganic filler, respectively. Dichloromethane (DCM) has been used as the solvent for PC, and solution casting method has been used to prepare PbO-filled PC composite films, with eleven different filler levels (FLs) which are expressed by weight fractions, ranging from 0.5 % up to 10 %. Lead (Pb) is a high-density material. Even though Pb is toxic in nature, it has many applications, especially for radiation shielding [46], and it is also used in light emitting diodes (LEDs), solar cells, photodetectors [47], coloring agents, plastic (in compounding materials), glass, oxidants, and bullets [48]. The production of EB radiation by the deceleration of electrons in composite films of PbO-filled PC has been studied, and the effective atomic number Z_{eff} of these composites have been determined by utilizing the obtained EB spectrum. The obtained values of Z_{eff} were compared with those of modified atomic number (Z_{mod}) which have been obtained theoretically, by using Markowicz and Van Grieken equation [49]. The Z-dependence on EB from PbO-filled PC composite has also been studied.

The EB study on these prepared (PbO-filled PC) composites has significance in the field of radiation shielding, where PbO-filled PC composites have been used as radiation shielding materials (for both beta and gamma radiation) [50] during transport of radioactive sources, in the preservation of radio active sources, in nuclear reactors, and in medical applications where there is a possibility to produce EB radiation by the deceleration of electrons.

METHODOLOGY

A thallium-activated sodium iodide (NaI(Tl)) scintillation detector has been used to conduct the experiments. The data acquisition process and analysis of the obtained spectra have been done by using Spectrum Acquisition and Analysis Software (SAAS). This detector includes a NaI(Tl) scintillator, which is coupled to a photomultiplier tube (PMT), a preamplifier (PA), and a linear amplifier (LA), followed by a personal computer

with multichannel analyzer (MCA), as illustrated in the block diagram presented in Fig. 1. After switching the detector on (gamma ray spectroscopy (GRS) instrument, used for energy spectroscopy), its energy was subsequently calibrated. Afterwards, its parameters such as applied high voltage, voltage gain, time period (time for which data is acquired) and lower level discriminator (LLD) value, were reset. Then, the data acquisition was started. The beta source $^{90}\text{Sr}/^{90}\text{Y}$ has been used as the radioactive source in order to conduct the experiment (EB study). Poly(methyl methacrylate) (PMMA) or Perspex sheets of suitable thickness have been used to attenuate the beta particles from ^{90}Sr . This arrangement makes it possible to get only the beta particles from ^{90}Y . Each spectrum has been acquired for 3600 seconds. The spectrum was obtained when the PMMA sheet of suitable thickness was placed at position 1 (P_1) which was between source and the target; this spectrum is only due to IB and the background.

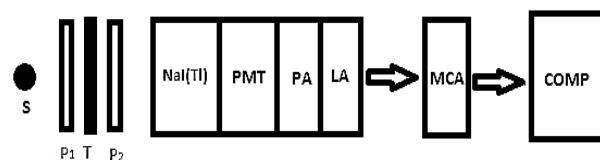


Fig. 1. A schematic block diagram of experimental setup for the EB study on PbO-filled PC composite films. Here S is source; P_1 and P_2 are the positions for placing the perspex sheets, for IB and EB, respectively; T is the target sample (material to be studied); NaI(Tl) is the thallium activated sodium iodide scintillation detector; PMT is photomultiplier tube; PA is preamplifier; LA is linear amplifier; MCA is multichannel analyzer and COMP is a Personal Computer or Laptop. High Voltage (HV) and Low Voltage (LV) units are present in the modular system, but not shown in the block diagram. For the portable setup, power is extracted and data is transferred through the USB port.

Due to placement of the PMMA sheet at position P_1 , all the beta particles from the source are attenuated by PMMA sheets, and therefore there are no beta particles passing through the target (sample). Thus, there is no EB radiation from the target. The recorded spectrum in this case is named Spectrum 1. When the PMMA sheets are placed in position 2 (P_2), which lies in between the target and the detector, the beta particles from radioactive source falls on the target (composite material). The particles interact with the target and produces EB. A spectrum consisting of EB, IB, and background is obtained; it is named Spectrum 2. The emission of EB in PMMA sheet is negligible when compared to in high-Z materials. Spectrum 2 is then subtracted from Spectrum 1. The resultant spectrum is the EB spectrum. The same procedure has been repeated for different absorber thicknesses (at each FL), and also

for films with different FLs. Figure 2 shows a photograph of the prepared PbO-filled PC composite films, which are used as targets in order to conduct the EB experiment.

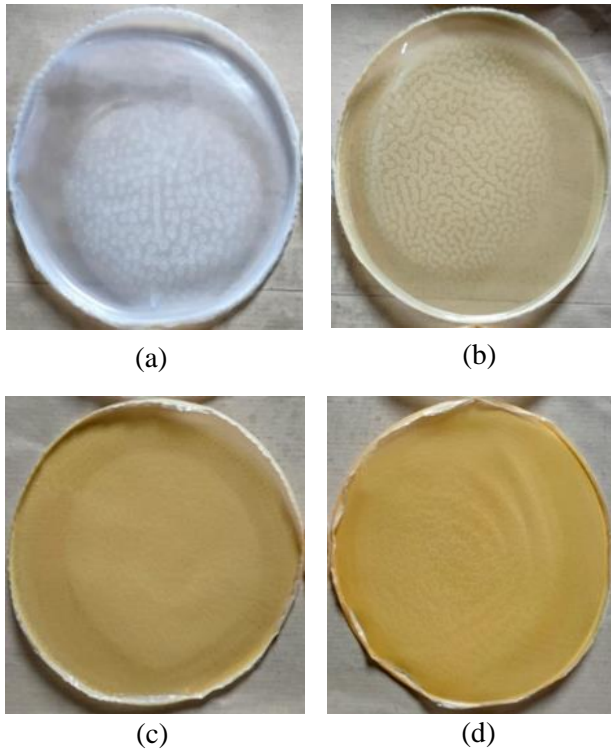


Fig. 2. Photograph of the prepared PbO-filled PC composite films for filler levels (FL), in terms of weight fraction, equal to (a) 0.0 %; (b) 2.5 %; (c) 5.0 %; and (d) 10 %.

RESULTS AND DISCUSSION

When beta particles (electrons having a continuous distribution of kinetic energy) from a radioactive source are incident on a material, they decelerate in the first few layers of the material, producing EB radiation. Then, they travel through the rest of the material (layers), and as they traverse the material, the intensity of the resulting EB gets reduced and the slowing down of beta particles takes place.

The modified atomic numbers (Z_{mod}) of the prepared composite material at each FL have been determined using Eq. (1) (Markowicz and Van Grieken equation) [49], and the determined value of Z_{mod} for all the prepared PbO-filled PC composites at different filler levels (FLs) are listed in Table 1.

$$Z_{mod} = \frac{\sum_i \frac{W_i Z_i^2}{A_i}}{\sum_i \frac{W_i Z_i}{A_i}} \quad (1)$$

Table 1. EB parameters related to PbO-filled PC composite films.

FL (%)	Z_{mod}	$-\Sigma_B$	$\ln(KZ^n)$	Z_{eff}
0.0	5.8358	0.018±0.0009	12.239±0.072	5.701±1.133
0.5	6.0699	0.016±0.0009	12.1178±0.073	6.159±1.135
1.0	6.3047	0.014±0.002	12.0423±0.158	6.462±1.193
2.0	6.7767	0.014±0.002	11.9974±0.204	6.649±1.228
2.5	7.0145	0.013±0.002	11.9123±0.099	7.028±1.154
3.0	7.2518	0.013±0.002	11.8026±0.171	7.525±1.205
3.5	7.4906	0.012±0.002	11.7624±0.136	7.720±1.180
4.0	7.7302	0.011±0.001	11.7358±0.118	7.851±1.169
5.0	8.2117	0.009±0.000	11.6769±0.067	8.151±1.137
8.0	9.6755	0.009±0.001	11.4110±0.151	9.651±1.194
10.0	10.668	0.008±0.001	11.2678±0.1280	10.57±1.181

In Eq. (1), W_i is weight fraction, A_i is mass number, and Z_i is the atomic number, respectively, of the i^{th} element present in the PbO-filled PC composite material.

The expression for the total intensity (I) of EB radiation produced in thick target of thickness t (in mg cm^{-2}), atomic weight A , atomic number Z and mass per unit area (expressed by ρt), is given by Eq. (2a) [51-52].

$$I = KZ^n \left(\frac{t}{A}\right) e^{-\Sigma_B t} \quad (2a)$$

In Eq. (2b), Σ_B denotes a material constant, while K is the proportionality constant (yield constant) which is independent of thickness (t) of the target, and it depends on EB cross section, intensity, energy of the beta emitter and the experimental setup. After rewriting Eqs. (2a,2b) is obtained.

$$\ln\left(\frac{IA}{t}\right) = \ln(KZ^n) - \Sigma_B t \quad (2b)$$

Eq. (2b) is the equation for a straight line. A graph of $\ln(IA/t)$ versus thickness of the target is plotted, and the data points are subjected to linear regression analysis. In other words, the slope and y-intercept were obtained by fitting the curve linearly. Here, the negative slope is Σ_B . The y-intercept is $\ln(KZ^n)$, the latter being the EB intensity per monoatomic layer of the thick target. Figure 3 illustrates the experimental determination of Σ_B and $\ln(KZ^n)$ for PbO weight fraction of 3.0 % in PC; the same procedure has been followed for all the composites (that is, at different FLs). The determined values are listed in Table 1, from which it is known that the atomic weight of prepared composite films decreases with increase in FL. It is well known that the mass attenuation coefficient (μ_m) of a high-energy photon quantifies the interaction of gamma radiation with matter, with the

involvement of such processes as photoelectric effect, Compton effect, and pair production, and these processes mainly depend on the atomic number of target materials, in addition to the energy of the incident gamma photons. Here, Σ_B is independent of the modified atomic number of the target, and it does not correspond to μ_m . From this fact, it can be concluded that the attenuation of low energy bremsstrahlung photons in the remaining layers of the thick target is not responsible for the nonlinearity in the increase of external bremsstrahlung intensity. Finally, Σ_B is independent of both Z_{mod} and end-point energy of the beta particles emitted from the radioactive source. The reason for nonlinearity in EB intensity may be the slowing down of beta particles in the course of its travel within the target. When the beta particles traverse the bulk of the target, it loses its energy by different processes such as diffusion, slowing down, excitation of atoms or molecules, and collision with target atoms (electrons of the target atoms), during which it may undergo deflection or scattering after each collision.

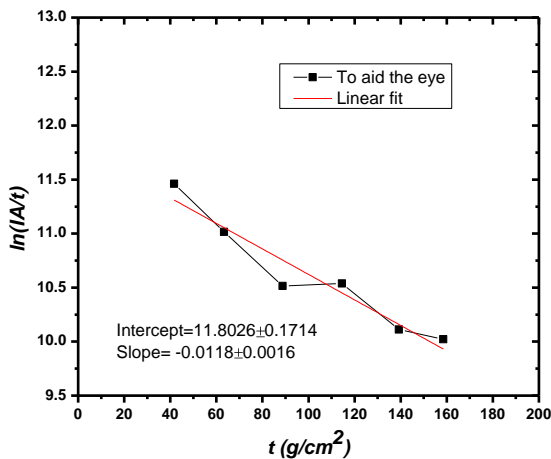


Fig. 3. Plot of $\ln(IA/t)$ versus thickness for PbO weight fraction of 3.0 %.

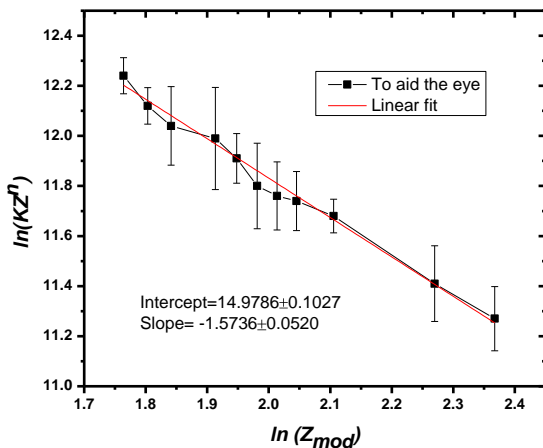


Fig. 4. The plot of $\ln(KZ^n)$ versus $\ln(Z_{mod})$, for all the PbO-filled PC composite films (at different FLs).

Figure 4 represents the plot of $\ln(Z_{mod})$ versus $\ln(KZ^n)$ at different FLs, and is noted that the resulting plot is linear. After linear least square fitting of the curve, the slope gives the index n and $\ln K$ is the y-intercept, and they are equal to 1.574 ± 0.052 and 14.978 ± 0.103 , respectively, as illustrated in Fig. 4.

Using $\ln(KZ^n)$ values of PbO-filled PC composite films, the Z_{eff} values were calculated for the same composite films by utilizing the obtained values of n and $\ln K$ by linear least squares fitting, and they were constant for the given targets used and for the geometrical set up utilized for acquiring data. This method is named the conventional intercept method [53].

The effective atomic number Z_{eff} is defined as the average number of electrons present in the material which are involved actively in the interaction. In order to determine Z_{eff} , several thicknesses of the same sample (targets) were used. Equation (3) is obtained from a modification of Eq. (2), and it is an equation for a straight line whose slope gives the index n and its y-intercept gives $\ln K$. By substituting all the known values for the quantities in Eq. (3), the Z_{eff} values for all the composite films at different FLs have been determined, and these are listed in Table 1.

$$\ln(KZ^n) = \ln K + n \ln Z \tag{3}$$

On comparing the values of Z_{eff} obtained from conventional intercept method with the Z_{mod} values obtained from Markowicz and Van Grieken equation, it is noted that there is a good agreement between these values, and therefore confirms the Z_{mod} values obtained for the prepared PbO-filled PC composite films. This also proves that the EB method is also a suitable method to determine Z_{mod} values for compounds.

From the plot of $\ln(Z_{mod})$ versus $\ln(KZ^n)$, after linear fit, the value of slope or the index is found to be equal to 1.574 ± 0.052 . This shows that the integrated external bremsstrahlung production per atom of the target is proportional to $Z^{1.574 \pm 0.052}$. This is approximately equal to Z^2 . Therefore, it indicates that the bremsstrahlung per atom varies as the square of the effective atomic number of the absorbing composite material.

CONCLUSION

PbO-filled PC composite films with different FLs have been used to study the production of EB radiation by the interaction of beta particles from

$^{90}\text{Sr}/^{90}\text{Y}$ radioactive source. It is seen that there is a nonlinearity in the increase in EB intensity with increase in target thickness, which depends on slowing of beta particles during the interaction with materials, but not on the attenuation of lower energy bremsstrahlung photons emitted in the first few layers of the stopping material. The EB study reveals that Σ_B is not dependent on either atomic number of the material or end point energy of beta particles. The EB spectrum intensity can be effectively used to obtain the value of Z_{eff} , and the values obtained are in good agreement with those of Z_{mod} obtained from the Markowicz and Van Grieken equation. The intensity of EB spectra depends on the square of the atomic number of the target material.

ACKNOWLEDGMENT

The authors acknowledge the use of weak radioactive sources, gamma ray spectrometer, and other required accessories available in the Postgraduate Laboratory of the Department of Physics, Karnatak University's Karnatak Science College, Dharwad in order to perform the measurements required for this work.

AUTHOR CONTRIBUTION

Vijayashri Ashok Kandagal performed the investigation, analysis and writing of the original draft, and Blaise Lobo supervised and performed editing and review of the written manuscript.

REFERENCES

1. R. Mirji and B. Lobo, J. Radioanal. Nucl. Chem. **324** (2020) 7.
2. O. V. Ogorodnikova, M. Majerle, J. Čížek et al., Sci. Rep. **10** (2020) 18898.
3. M. Yücemöz and M. Füllekrug, J. Geophys. Res.: Atmos. **126** (2021) e2020JD033204.
4. P. Montay-Gruel, S. Corde, J. A. Laissue et al., Med. Phys. **49** (2022) 2055.
5. A. V. Korol and A. V. Solov'yov, Polarization Bremsstrahlung, Vol. 23, Springer, Berlin (2014) 1.
6. D. Mrdja, K. Bikit, I. Bikit et al., J. Radiol. Prot. **38** (2017) 34.
7. R. D. Evans, *Radiative Collisions of Electrons with Atomic Nuclei*, in: The Atomic Nucleus Vol. 582, McGraw-Hill Book Company, India (1955) 600.
8. A. S. Dhaliwal, Nucl. Instrum. Methods Phys. Res., Sect. B **234** (2005) 194.
9. G. Haridas, D. Verma, P. K. Sahni et al., Indian J. Pure Appl. Phys. **50** (2012) 462.
10. M. F. L'Annunziata, *Electromagnetic Radiation: Photons*, in: Radioactivity Introduction and History, from the Quantum to Quarks, 2nd ed., Elsevier, Netherlands (2016) 278.
11. G. H. Aston, *The Amount of Energy Emitted in the γ -ray Form by Radium E*, Mathematical Proceedings of the Cambridge Philosophical Society **23** (1927) 935.
12. J. K. Knipp and G. E. Uhlenbeck, Phys. **3** (1936) 425.
13. F. Bloch, Phys. Rev. J. Arch. **50** (1936) 272.
14. C. S. W. Chang and D. L. Falkoff, Phys. Rev. J. Arch. **76** (1949) 365.
15. S. B. Nilsson, Ark. Fys. **10** (1956) 467.
16. L. Spruch and W. Gold, Phys. Rev. J. Arch. **113** (1959) 1060.
17. R. R. Lewis and G. W. Ford, Phys. Rev. **107** (1957) 756.
18. G. W. Ford and C. F. Martin, Nucl. Phys. A **134** (1969) 457.
19. A. Sommerfeld, Ann. Phys. **403** (1931) 257.
20. F. Sauter, Ann. Phys. **412** (1934) 404.
21. G. Racah, Il Nuovo Cimento. **11** (1934) 461.
22. H. Bethe and W. Heitler, *On the Stopping of Fast Particles and on the Creation of Positive Electrons*, Proceedings of the Royal Society of London Series A: Mathematical, Physical and Character. **146** (1934) 83.
23. H. K. Tseng and R. H. Pratt, Phys. Rev. A **3** (1971) 100.
24. S. M. Seltzer and M. J. Berger, At. Data Nucl. Data Tables 35, Elsevier (1986) 345.
25. B. L. Dekker, M. H. Links, A. C. M. Kobold et al., J. Clin. Endocrinol. Metab. **107** (2022) e604.
26. C. J. Montaña and T. P. R. D. Campos, Acta Ortop. Brass. **27** (2019) 64.
27. R. Padovani and C. Deehan, *Radiation Interaction and Dosimetry*, in: Introduction to Medical Physics, 1st ed., CRC Press (2022) 15.
28. P. Taherparvar and N. Shahmari, Nucl. Med. Rev. **22** (2019) 45.

29. C. İnce, Ö. Karadeniz, T. Ertay *et al.*, (2021). *Appl. Radiat. Isot.* **167** (2021) 109453.
30. D. Carlotti, F. Collamati, R. Faccini *et al.*, *J. Instrum.* **12** (2017) 11006.
31. A. Ho, S. S. H. Witharana, G. Joonkmans, *Radiat. Prot. Dosim.* **151** (2012) 443.
32. V. G. Rudychev, M. O. Azarenkov, I. O. Girka *et al.*, *Probl. At. Sci. Technol.* **138** (2022) 98.
33. M. Kim, J. K. Bae, B. H. Hong *et al.*, *Nucl. Eng. Technol.* **51** (2019) 539.
34. I. Meleshenkovskii, T. Ogawa, A. Sari *et al.*, *Nucl. Instrum. Methods Phys. Res., Sect. B* **483** (2020) 5.
35. B. Budick, J. Chen and H. Lin, *Phys. Rev. C.* **46** (1992) 1267.
36. Z. Yu, Y. Bai, J. H. Wang *et al.*, *Energy Environ.* **12** (2021) 66.
37. V. D. Jadhav, A. J. Patil and B. Kandasubramanian, *Polycarbonate Nanocomposites for High Impact Applications. Handbook of Consumer Nanoproducts*, in: *Handbook of Consumer Nanoproducts*, Springer, Singapore (2022) 1.
38. R. Mirji and B. Lobo, *J. Radioanal. Nucl. Chem.* **324** (2020) 7.
39. N. A. A. B. Taib, M. R. Rahman and M. K. B. Bakri, *Cellulose Reinforcement in Thermoplastic Composites*, in: *Fundamentals and Recent Advances in Nanocomposites Based on Polymers and Nanocellulose*, Elsevier (2022) 103.
40. A. Ganguly, P. Channe, R. Jha *et al.*, *Polym. Eng. Sci.* **61** (2021) 650.
41. I. Blanco, G. Cicala, G. Ognibene *et al.*, *Polym. Degrad. Stab.* **154** (2018) 234.
42. K. Sushmita, G. Madras and S. Bose, *Funct. Compos. Mater.* **2** (2021) 1.
43. A. Hassan, O. E. Ezenkwa, A. S. Ismail *et al.*, *PERINTIS eJournal* **9** (2019) 1.
44. A. S. Swinarew, B. Swinarew, T. Flak *et al.*, *Polym.* **13** (2021) 3572.
45. R. Mirji and B. Lobo, *Opt. Mater.* **113** (2021) 110862.
46. K. Bagheri, S. M. Razavi, S. J. Ahmadi *et al.*, *Radiat. Phys. Chem.* **146** (2018) 5.
47. L. Gao and Q. Yan, *Sol. RRL* **4** (2020) 1900210.
48. M. Boldyrev, *Wiki J. Sci.* **1** (2018) 7.
49. M. C. Koramar and B. Lobo, *Radiat. Prot. Dosim.* **199** (2023) 1248.
50. V. A. Kandagal, R. Mirji and B. Lobo, *Mater. Today Proc.* **49** (2022) 2212.
51. T. S. Mudhole and N. Umakantha, *Am. J. Phys.* **40** (1972) 591.
52. C. S. Mahajan, *Sci. Res. Rep.* **2** (2012) 152.
53. M. V. Manjunatha, B. M. Sankarshan and T. K. Umesh, *X-Ray Spectrom.* **43** (2014) 246.